J Mater Sci (2008) 43:6695–6703
DOI 10.1007/s10853-008-2689-8

Enhancement of composite scarf joint interface strength through carbon nanotube reinforcement

Y. W. Kwon · R. Slaff · S. Bartlett · T. Greene

Received: 18 March 2008 / Accepted: 30 April 2008 / Published online: 31 July 2008

Abstract It was investigated whether there was a potentially significant improvement to scarf joint bonding that was achieved through the dispersion of carbon nanotubes (CNTs) along the interface of the composite joint. The study examined various factors that might affect CNT-reinforced joint interface strength. Each composite joint consisted of a vinylester matrix base (DERAKANE 510-A) interlaced with a carbon fiber weave (TORAY T700CF). During the curing process, the research explored several variables concerning the CNT application. The testing included single-walled CNTs (SWCNT), and conventional and bamboo-structure multi-walled CNTs (MWCNT) with varying length, purity, and concentration levels along the surface area of the joint interface. This wide array of data demonstrated the effect of CNTs introduction at the joint interface, and provided the ideal type, size, purity level, and concentration level for composite scarf joint bond reinforcement using CNTs. Furthermore, a computational model was developed to predict the strength of the scarf joints. The predicted model agreed well with the experimental data.

Introduction

Modern ship construction is continually gravitating toward composite structures that ideally reduce weight without sacrificing strength. The endeavor to construct the entire superstructure of the next generation destroyer solely of composites has raised many questions regarding joint strength at composite interfaces. The composites themselves are sufficiently strong [1]. However, there are inherent weaknesses present at adjoining sections due to the break in continuity of fibrous material. At these joints, the structures are more susceptible to failure. The joint interface lacks the strength characteristics possessed by the remainder of the composite section. It is this discontinuity in fibrous material that deprives the structure of the additional strength characteristics attributed to the fiber. The question is, since there is no easy way to avoid the fiber discontinuity, how can the strength of the joint be enhanced enough to consistently support loaded conditions?

The emergence of the carbon nanotube (CNT) and the benefits of its properties have opened many possibilities for structural enhancement. For over a decade, the primary research in this area has dealt with nanotube inclusion directly into composite material. The elastic modulus of CNTs is greater than 1 TPa, and 10–100 times stronger than the strongest steels, with tremendous reductions in weight [2]. This attribute possessed by CNTs has made them extremely desirable for use in composite reinforcement. Countless studies have been performed using CNTs to reinforce different matrix materials including ceramics, metals, and polymers. In some studies, different types of CNT's were tested in the same polymer matrix. One study documented the use of several different types of CNTs in a polymer composite, yielding a twofold increase in Young's modulus. The same study indicated that smaller diameter multi-walled CNTs (MWCNTs) were the ideal CNT for reinforcement due to their surface area characteristics [3].

Improvements in stiffness and strength, through the inclusion of CNTs, have been proven over and over again.

Y. W. Kwon (✉) · R. Slaff · T. Greene
Department of Mechanical and Astronautical Engineering,
Naval Postgraduate School, Monterey, CA 93943, USA
e-mail: ywkwon@nps.edu

S. Bartlett
Carderock Division, Naval Surface Warfare Center,
West Bethesda, MD 20817-5700, USA

The general conclusion is that in order to harness the strength characteristics of the CNT, CNT/matrix wetting, adhesion, and uniform CNT dispersion are of extreme importance. Wetting and adhesion are most important because in order for the reinforcement to be effective, strong interfacial bonding must be present [2]. Wettability is the ability of the composite matrix to contact the surface of the reinforcement. The interfacial bonding will provoke load transfer between CNTs and polymers. With load transfer being imperative to the success of strength enhancements, numerous studies have been performed to analyze the CNT polymer interface. Micromechanical interlocking, chemical bonding, and van der Waals bonding between the fiber and the matrix are the three mechanisms of load transfer. With van der Waals bonding being weak and micromechanical interlocking being improbable due to the CNT's inherent smooth surface, chemical bonding is the most influential mechanism in nanotube load transfer [4]. Following this observation, studies were performed in attempts to quantify the chemical bonding [5]. These studies support the chemical bonding hypothesis which explains the interfacial bonding strength and ultimately helps to gain understanding as to why CNT reinforcement of polymers is generally a success [6]. Another study [2] showed various CNT pullout positions as the polymer fractures. It also indicated the crack bridging of CNTs following crack initiation.

The topic of the present research is not to investigate interfacial bonding strength or the strength improvements of CNT-reinforced composites. Those topics have been investigated extensively and proven positive. This study builds off of the already known CNT-polymer strength enhancements. The costs of CNTs make them impractical for many naval construction applications. However, if they could be used in a local application to improve the weakest points in a composite structure, then they could reinforce the structural weak points without the added expense of dispersing nanotubes throughout the matrix. This study explores the possibility of localized reinforcement of a weak point, the scarf joint, in order to prove that CNT's can reinforce isolated positions without conventional dispersion methods.

The research objective was to investigate the effect that CNT dispersion along the joint interface has on scarf joint strength. The study examined various factors that could affect joint strength along with CNTs. The study focused on determining the optimal parameters to improve the interface strength significantly.

The wide array of testing was conducted to conclusively demonstrate the effect of the introduction of CNTs to the interface of a composite joint. If there was a substantial increase in joint strength, it should be related to several variables. The variables included, CNT dispersing agents, types of CNTs (single-wall, conventional-type, or bamboo-type multi-wall), length of nanotubes, diameter of CNTs, and concentration of nanotubes across the surface of the joint interface. Furthermore, a computational modeling technique was developed and applied to predict the failure strength of the scarf joints. The predicted results were compared to the experimental data for validation of the computational model.

Preparation of scarf joint specimens

The composite test joints were constructed via a vacuum bag layup procedure with an overlap in the joint interface as sketched in Fig. 1. A step–step interface configuration was used due to the ease of CNT application and to alleviate some of the construction complications. The composite consists of a vinyl-ester matrix base (Derakane 510A) with carbon fiber (Toray T700 CF) plain weave fabrics.

CNTs were applied along the joint interface because the majority of non-buckling failures under a tensile or compressive load occur at that location [1]. The nanotube application was designed to reinforce the inherent weak spot in joint construction. The benefits of CNT-reinforced polymers have been documented on several occasions. For example, an epoxy-based polymer matrix composite recorded an increase in modulus and strength in both tension and compression [7].

Scarf joint construction procedure with CNTs

Once the proper procedure for composite construction was identified, the procedure was standardized to ensure each test sample was constructed in the same fashion. Each sample consisted of 16 plies of Toray T700 carbon fibers that combine to form a four-step interface as shown in Fig. 1. Each step consisted of four plies of carbon fiber fabric. The total thickness of each test joint was $\sim$0.9 cm. The length of each step was $\sim$1.3 cm. This generated an overall joint interface of 3.8 cm with an overlap of $\sim$1.3 cm. The resulting aspect ratio, interface length (L) divided by overall thickness (t), was approximately equal to 4.0.

The step-by-step process has been articulated and illustrated below.

Step 1: Cut 16 sheet of carbon fiber fabric such as four sheets 25.4 cm $\times$ 17.2 cm, four sheets 25.4 cm $\times$ 15.9 cm,

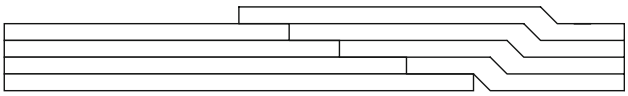

Fig. 1 Layup configuration

four sheets 25.4 cm × 14.6 cm, and four sheets 25.4 cm × 13.3 cm.

Step 2: Manually apply resin compound to each sheet of carbon fiber fabric using a brush. A layer of porous non-permeable ply and peel ply should be spread across the aluminum plates prior to composite layup.

Step 3: While applying the resin to the reinforcement, be sure to align sheets to produce four steps with an individual step interface length of 1.3 cm.

Step 4: Immediately following the completion of the 16 ply layup, the composite should be wrapped in one layer of peel ply, followed by one layer of porous non-permeable ply, followed by one layer of buffer ply.

Step 5: After the application of the various plies, the plate should be placed inside the vacuum bag. Seal the bag and ensure that it is airtight.

Step 6: Connect the vacuum to the bag and turn the vacuum on. This removes the excess air in the bag and reduces the trapped air in the composite structure. The negative pressure created by the vacuum also promotes the removal of excess resin which is consequently absorbed by the buffer ply.

Step 7: After 8 h of curing, turn off the vacuum, remove aluminum plate from the bag, and remove the top plies. Half of the test joint plate has been constructed.

Step 8: Spread the dispersed nanotubes in solution across the step interface of the composite plate base.

Step 9: Allow dispersing agent to evaporate leaving only the CNTs at the joint interface.

Step 10: Repeat Steps 1 through 6 along the step interface of the completed half. Ensure the top four sheets of carbon fiber create an overlap at least 1.3 cm in length. Figure 2 shows a prepared composite sheet before curing.

Step 11: After 8 h of curing, remove all plies from the top and bottom of the composite joint plate. The composite plate is now ready for sample preparation.

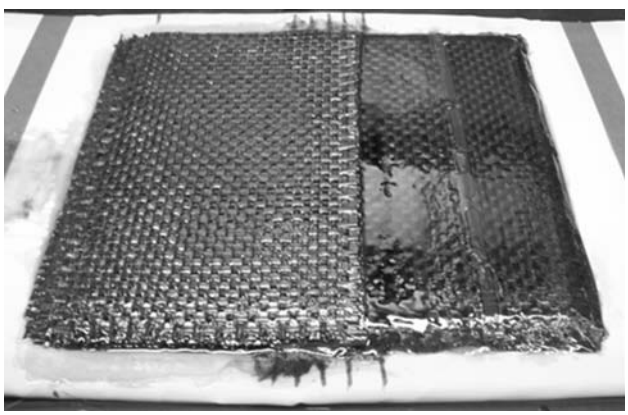

Fig. 2 Prepared composite scarf joint sheet before curing

Testing phases with differently prepared specimens

There were three phases of testing in order to determine the effect of each individual factor associated with CNT's. Testing was conducted sequentially from the first test phase because the results of the present test phase were used to guide the next phase of test. Each phase of testing is described below.

Phase 1: dispersion agent

Although control of CNT orientation was not possible for this experiment, an effort was made to increase CNT wettability which in turn could potentially increases the interface bonding strength between the CNT and the matrix. The CNTs were initially dispersed separately in both ethylene glycol and acetone to determine which one was a better dispersing agent.

The CNTs show better dispersion characteristics in the ethylene glycol. However, the ethylene glycol leaves a slight residue after being allowed to evaporate for 24 h. The CNTs did not disperse quite well in the acetone. However, the acetone did evaporate, residue free, in <10 min. Acetone also possesses another property that must be considered. Acetone has the potential to chemisorb on nanotubes. CNTs that possess defects are more susceptible to the chemisorption and thereby could potentially change the surface character and consequently the strength characteristics of the defective CNTs. During the dispersing agent comparison, 0.15 g of MWCNT (diameter = 20–40 nm, length = 10–30 nm, purity > 95%) was dispersed across an area of 5.08 cm × 25.4 cm for a surface area concentration of ∼11.5 g/m^2.

Phase 2: surface area concentration

Following the resolution of the better dispersing agent, surface area concentration was varied to determine the effect of different application amounts to the 5.08 cm × 25.4 cm joint interface. Two different concentration levels were tested. The type of nanotube that was used was a high quality, 95% pure MWCNT, with a length of 1–5 μm, and a diameter of 15 ± 5 nm. The amounts of MWCNT that were used in this phase of experimentation were 0.15 and 0.10 g, which provided concentration levels of ∼11.5 and 7.5 g/m^2, respectively. A set of samples without nanotube reinforcement were also constructed in order to provide a basis for comparison.

Phase 3: CNT types and sizes

After determining the ideal dispersing agent and concentration level, the final phase of experimentation varied

Table 1 List of scarf joint specimens containing different CNTs

Group name	Description of nanotube structures
SWCNT	Single-wall CNTs, outer diameter 1–1.5 nm, length 1–10 μm, purity > 80%
MWCNT-A	Multiwall-CNTs, outer diameter 30 ± 15 nm, length 1–5 μm, purity > 95%
MWCNT-B	Multiwall-CNTs, outer diameter 25 ± 5 nm, length 10–30 μm, purity > 95%
MWCNT-C	Multiwall-CNTs, outer diameter 15 ± 5 nm, length 5–20 μm, purity > 95%
MWCNT-D	Multiwall-CNTs, outer diameter 30 ± 15 nm, length 5–20 μm, purity > 95%
MWCNT-E	Bamboo-structured multiwall-CNTs, outer diameter 30 ± 15 nm, length 1–5 μm, purity > 95%
MWCNT-F	Bamboo-structured multiwall-CNTs, outer diameter 30 ± 15 nm, length 5–20 μm, purity > 95%

several CNT characteristics, in order to attempt to discern the effect those characteristics had on interface strength. CNTs of different types and sizes were tested in this phase.

The CNTs were produced using the chemical vapor deposition process. Single-walled, conventional multi-walled, and bamboo-structured MWCNTs of various lengths and diameters were tested. Bamboo-structured nanotubes are discontinuous along the length and have many edge sites for functionalization. Functionalization is the process of physically or chemically attaching in molecules (functional groups), to the wall of an imperfect CNT without significantly changing the nanotubes' desirable properties. This makes CNTs more easily dispersible in liquids. Table 1 lists a list of the CNTs that were tested. The three phases of testing, previously described, were designed to determine the optimum combination of dispersing agent, surface area concentration, and CNT type for composite joint reinforcement.

Experimental setup and testing

The composite scarf joints were fabricated in accordance with the steps outlined previously. The scarf joints were constructed in sheets. The sheets were cut into test specimens by using the Jet Edge Waterjet cutter. Each specimen was 24.0–24.2 cm in length and 3.8–3.9 cm in width. Since the layup procedure for constructing the sheets was standardized, the thickness for each specimen was always between 0.8 and 0.9 cm. This provided a sample transverse cross-sectional area of 3.0–3.5 cm^2.

Each sample was set up the same for testing. They were mounted longitudinally in the Instron Tension/Compression Machine (Model Number: 4507/4500) with a 100-kN load cell. The samples were clamped ~6 cm from each end. This provided an effective test joint length of 12.0–12.1 cm between the top and the bottom clamps. Since the samples were to be loaded in compression, aluminum blocks were wedged between the surface of the clamp and the end of the sample. These wedges prevented the samples from splintering at the ends which ensured that the failure of the test joint would occur along the joint interface.

Once the sample was set up correctly, the computer program Series IX was enabled to control the load and record the data. The recorded data included applied compressive load and displacement. The program required manual input of each sample length, width, and thickness to ensure the proper stress versus strain relationships were calculated.

While the stress versus strain relationships was being tabulated, the crack initiation and propagation were observed using high-speed video equipment. The high-speed camera was set at 1,500 frames per second with additional light fixtures rigged to illuminate the sample. The purpose of this aspect of experimentation is to discern whether or not there is a difference in crack initiation and propagation between non-reinforced and CNT-reinforced joint interfaces.

Results and discussion

Phase 1 tests

Phase 1 experimentation consisted of two sets of CNT-reinforced test samples. The CNTs were dispersed separately in both ethylene glycol and acetone to determine which one was the better dispersing agent. There was another set of test joints constructed without CNT reinforcement in order to provide a basis for comparison between samples with and without CNT reinforcement. The three specimens were tested for each case. Each test sample fractured at the expected location along the diagonal step interface of the joint. An example of the failure is shown in Fig. 3. The average results of the three tests are shown in Fig. 4 as well as their standard deviation imposed on the bar graph.

Based on the results, one can conclude that the acetone is the better choice for a dispersing agent. The acetone case exhibited more than a 50% greater capacity for maximum

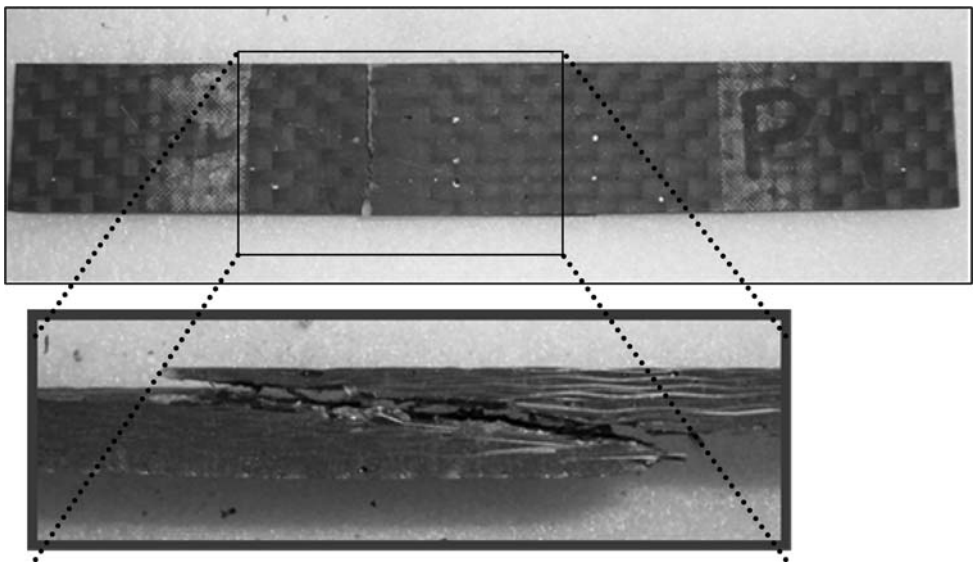

Fig. 3 Tested joint failure location

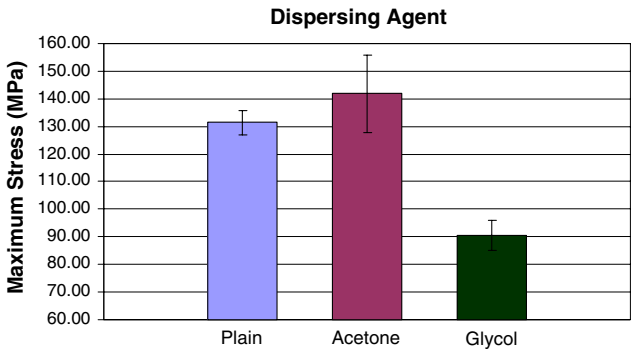

Fig. 4 Comparison between two different CNT dispersing agents

stress than the glycol case. Based on the slope of the stress versus strain curves, the modulus of elasticity for the acetone-nanotube solution was more than 45% greater than the ethylene glycol-nanotube solution.

There were also encouraging results when comparing the data from the acetone-nanotube solution to that of from the plain specimens without CNTs. There was an observed 5–10% increase in maximum stress and elastic modulus. Despite these encouraging numbers, the data do not conclusively determine an enhancement of joint interface strength because of the closeness of the two data sets, i.e., the large standard deviation for the acetone case, and the small number of test samples. The final determination of strength enhancement will be examined in Phase 3 tests.

Phase 2 tests

Phase 2 experimentation consisted of two sets of CNT-reinforced test samples with different surface area concentrations. The CNTs were dispersed using acetone as the dispersing agent based on the results from Phase 1. The concentration levels tested were 7.5 and 11.5 g/m^2. Based on

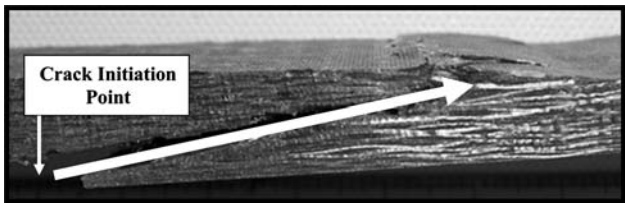

Fig. 5 Crack initiation at the bottom end of the joint and propagation toward the other end

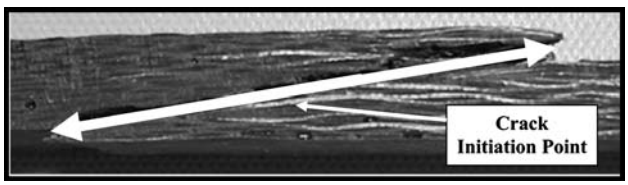

Fig. 6 Crack initiation in the middle of the joint and propagation toward both ends

the size of the composite sheets that were constructed and the 4:1 aspect ratio along the joint interface, the amounts of CNTs used per sheet were 0.10 and 0.15 g, respectively. There was another set of test joints constructed without CNT reinforcement in order to provide a basis for comparison between samples with and without CNT reinforcement. Four test specimens were used for each case.

Almost every test sample fractured at the expected location along the diagonal step interface of the joint. During testing there was a trend in crack initiation and propagation that was observed. For the majority of test joints, the crack initiated either at the base of the bottom step or at the center of the joint and propagated diagonally along the joint interface. An example of each failure mode is shown in Figs. 5 and 6. Fracture initiation and propagation was explored further in Phase 3 using high-speed video equipment.

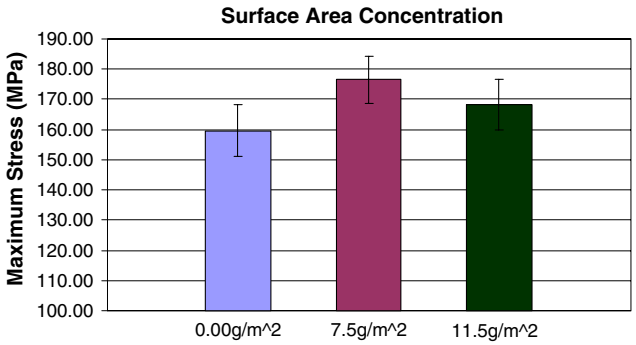

Fig. 7 Comparison of different CNT surface area concentrations

The average failure stress for each group of test samples is shown in Fig. 7. The figure shows the standard deviation of the data as well, in order to gain a greater understanding of the trends and data consistency that is prevalent in the results.

It was evident from Fig. 7 that the surface area concentration of CNTs did affect the strength of the composite joint. Both the 7.5 and the 11.5 g/m^2 concentration levels resulted in a strength increase over the non-reinforced composite joints. The greatest increase occurred with the 7.5 g/m^2 concentration level which revealed an improvement in joint strength of 10.6%. This percentage was almost double the strength improvement witnessed by the 11.5 g/m^2 concentration level.

Even more importantly, the inclusion of the standard deviation shows no overlap between the results of the non-reinforced and the results of the 7.5 g/m^2 CNT-concentration level. This proves not only that the 7.5 g/m^2 concentration level is superior to 11.5 g/m^2, but also that the CNT reinforcement has a definite positive impact on composite scarf joint strength. As shown in Fig. 7, even the lowest observed maximum stress in the 7.5 g/m^2 data set is greater than every observed value of maximum stress of the non-reinforced data set.

Phase 3 tests

Phase 3 experimentation consisted of eight sets of test samples. One set of samples was constructed without CNT reinforcement to provide a basis for comparison. A second set of test joint was constructed with single-walled CNTs (SWCNTs). The remaining six sets of test joints were constructed with different types of MWCNTs as listed in Table 1.

MWCNT groups A, C, D, E, and F along with the SWCNT were all ordered through the same vendor. The nanotubes used in Group B were ordered through a separate vendor at one-fourth the cost for CNTs of similar size and purity. MWCNT B was an economic alternative to the other MWCNT.

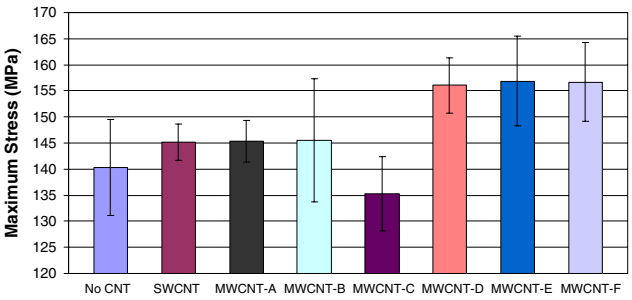

Fig. 8 Comparison of different kinds of CNT reinforcements

The CNTs were applied using acetone as the dispersing agent based on the results from Phase 1. The surface area concentration level used for each set of reinforced test samples was 7.5 g/m^2 based on the results from Phase 2. Based on the size of the composite sheets that were constructed and the 4:1 aspect ratio along the joint interface, the amount of CNT used for reinforcement was 0.10 g per sheet. Five specimens were tested for each type of CNT, and the results of each test were used with the exception of the Sample #4 of MWCNT Group E, which yielded poor data due to improper setup.

Figure 8 shows the average maximum stress for each case. Each case is plotted in conjunction with their respective standard deviation to show the consistency of the data sets. Table 2 shows the comparison of elastic moduli of different CNT-reinforcement cases.

Phase 3 observed maximum stress values lower than the stress values observed in Phase 2 in every case including the non-reinforced, which was constructed in both phases. The potential cause for the difference could be the shelf life of the resin. Phase 2 was constructed when the resin was 4 month old, while Phase 3 was constructed when the resin was five and a half months old. The strength properties of the resin begin to degrade after $\sim$4 months. The non-reinforced specimens were constructed first in Phase 3 in order to ensure that the results were not biased toward the reinforced specimens due to the aging resin.

Each group provided a joint strength increase, compared to the non-reinforced specimens, with the exception of Group C. The greatest strength increase was observed by Groups D–F. All three of those groups demonstrated an average strength increase of greater than 11%. Of these three groups, it appears as though Group D possesses the best strength enhancement characteristics. It had greater than an 11% increase in strength and possessed the most consistent data of the three top reinforcements. This consistency can be seen by observing the standard deviations shown in Fig. 8.

Groups E and F are bamboo-type CNTs. They have regularly occurring compartment-like graphitic structures inside the nanotube similar to the bamboo plant [8]. These

Table 2 Comparison of elastic moduli of different CNT reinforcement cases

	No. CNT	SWCNT	MWCNT-A	MWCNT-B	MWCNT-C	MWCNT-D	MWCNT-E	MWCNT-F
Elastic modulus (MPa)	64.6	73.6	81.5	75.4	70.9	74.4	74.4	69.2

types of CNTs were used with the notion that the compartment-like graphitic structures could provide additional support when used for reinforcement and the open ended molecular structure of the multi-walled bamboo-type CNT would increase wettability and functionalization. This would allow for increased interfacial bonding which would in turn increase the load transfer between the resin and the CNT which would ultimately improve the joint interface strength of the composite structure. The strength increase indicated in Fig. 8 confirms that the bamboo structure has better strength characteristics compared to conventional CNTs of similar size and purity when Group A results compared to Group E results.

Group B, the economic option, had some samples that provided strong reinforcement and others that were actually weaker than the non-reinforced specimens. As a result the average strength was greater than the non-reinforced samples, but the standard deviation was quite large. The standard deviation of group B was almost 30% larger than any other group. All MWCNT groups were 95% pure, but perhaps the economic option might have lower quality control.

The modulus of elasticity increased dramatically in every case. The greatest increase came with Group A which displayed over a 26% increase in modulus compared to the test joints without CNT reinforcement. Of the three groups that had the greatest strength increase, D–F, groups D and E each had modulus increases >15%. Group F had the lowest impact of all the groups with increase in modulus of just over 7%.

The majority of test sample fractured at the expected location along the diagonal step interface of the joint. The trends in crack initiation and propagation observed in Phase 2 were verified in Phase 3 using a high-speed camera. The majority of test joints initiated cracks either at the base of the bottom step or at the center of the joint and propagated diagonally along the joint interface.

There was one other type of fracture that rarely occurred, where the crack propagation did not follow the path of the joint interface. The crack initiated at the base but instead of propagating along the interface, it propagated along the undulated section of the samples. Figure 9 shows the direction of failure.

This alternative fracture phenomenon did not happen until Phase 3. In Phase 3 only one group had consistently these types of fractures. Group D had every test joint failure along the alternative line of fracture. This group

Fig. 9 Alternative failure direction for specimens of MWCNT-D

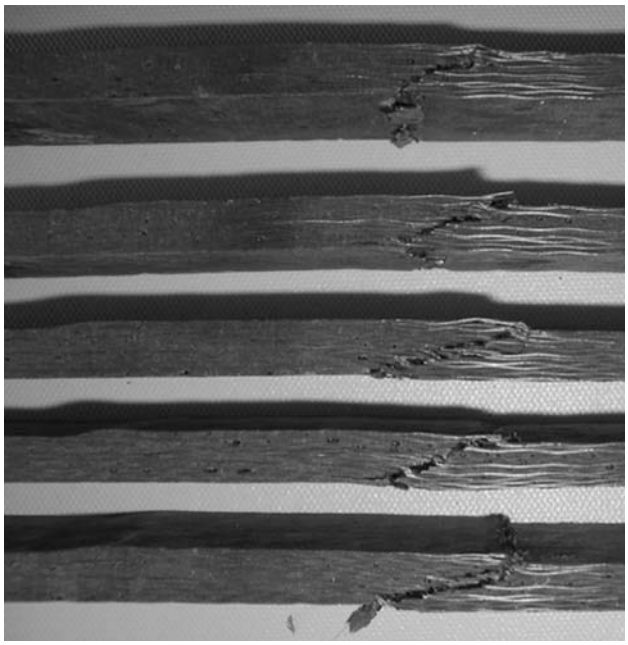

Fig. 10 Consistent failure group MWCNT-D specimens

also happened to have the most consistent strength enhancement and the highest elastic modulus of the three top CNT reinforcements. Figure 10 shows all five test joints in this group with the same mode of fracture.

A possible explanation for the consistency of this failure in Group D is that the CNTs provided enough of an enhancement in strength along the joint interface that the interface ceased to be the weakest portion of the specimen. Instead, the samples failed along second weakest portion of the joint, the step down created by the overlap associated with the composite construction. This type of failure mode was associated with localized fiber buckling.

Computational modeling and simulation

A computational model was used to predict the failure strength of the composite scarf joints. A multilevel technique was used in the computer model. First of all, a global

Fig. 11 Global–local finite-element model

model was analyzed, which represented the whole specimen including the scarf joint as shown in Fig. 11. Then, a local model was considered. The displacement boundary condition of the local model was obtained from the global model. The local model was constructed around the bottom section of the scarf joint as sketched in Fig. 11. In the local model, the resin layer was modeled discretely because the failure of the scarf joint was considered as the delamination along the resin layer. The triangular zone shown in Fig. 11 indicates the zone containing the resin layer. Because the global model did not include the resin layer discretely, the resin layer zone was modeled as a triangular shape so that it disappeared at the boundary of the local model. Therefore, the boundary of the local model was consistent with the global model.

In order to determine the failure strength, an initial flaw or a crack was assumed at the edge of the resin layer. The flaw size was selected to be smaller than the length detectable with a modern instrument. The assumed size was 0.0241 cm. Under compressive loading, the crack propagation was the shearing mode (i.e., mode 2) only because there was no crack opening. Furthermore, a previous study [9] showed that a crack assumed in the inclined orientation at the same slope of the scarf taper ratio, which was defined as the specimen thickness divided by the length of the scarf section, resulted in more reliable solutions. By doing so, the effect of the scarf taper ratio was accounted into the model. In addition, the study [9] indicated that use of the homogeneous smeared material properties in the global and local models except for the resin layer was acceptable in terms of the accuracy of the results and the simplicity of the models. As a result, the same techniques were used for the present study.

Finally, in order to predict the failure strength of the scarf joint, the energy release rate was computed from the initial crack. Then, the failure load was calculated such that the computed energy release rate became the critical energy release rate of the resin layer. The energy release rate for mode 2, G_{II}, was computed from the following equation:

$$G_{II} = \frac{1}{2} F \frac{\Delta u}{\Delta a}, \tag{1}$$

where F is the tangential force at the crack tip node, Δu the tangential relative displacement of the crack tip node caused by the crack tip movement Δa. Once the energy release rate was computed for a unit force applied to a specimen, the joint failure strength P_{fail} was computed from

$$P_{fail} = \sqrt{\frac{G_{IIc}}{G_{II}}}, \tag{2}$$

where G_{II} is the energy release rate computed for the unit applied force. In Eq. 2, it was considered that once the crack grew, it would lead into the complete failure of the scarf joint. This was observed during the physical testing of scarf joint failure.

The computed joint strength was compared to the failure strength obtained from the test. This comparison was performed for the scarf joint without CNTs because the fracture toughness of the resin layer with CNTs is not available at that time. These properties will be obtained in a subsequent study. The predicted compressive failure strength was 58 kN, while the average failure load from the experiment was 56 kN with the standard deviation of 3.16 kN. They agreed very well each other. This indicated the computational model was acceptable for predicting the failure load of the scarf joint under compression.

Summary and conclusions

This research investigated many aspects of CNT reinforcement of the vinyl-ester resin, Derakane 510A at the scarf joint interface. Phase 1 concluded that acetone was a better dispersing agent compared to ethylene glycol. The acetone dispersion proved to be greater than 50% stronger than the ethylene glycol dispersion. This was due in part to the acetone evaporating residue free compared to the ethylene glycol.

Phase 2 investigated the effect of CNT surface area concentration. This phase proved that the reinforcement benefits provided by localized application of CNTs were dependent upon surface area concentration. The dependency on surface area concentration was proven by testing samples with concentration levels of 7.5 and 11.5 g/m^2. The comparison revealed that a 7.5 g/m^2 surface area concentration was stronger compared to 11.5 g/m^2. The lower concentration level provided better CNT spacing which increased wettability and in turn increased CNT interfacial bonding with the vinyl-ester resin.

This phase also showed conclusively that localized reinforcement of composite scarf joints with CNTs worked. The reinforced test samples were $\sim$10% stronger than the non-reinforced and the standard deviations of both data sets remained outside one another. Since only two concentration levels were tested, the optimal level is unknown and it will be determined in a subsequent work. The conclusions from Phases 1 and 2 allowed for a refined investigation of the optimal type of CNT to be used for reinforcement.

From the data accumulated throughout Phase 3, there were a myriad of conclusions that could be reached. First

and foremost, the phase accomplished its purpose to identify the ideal type of CNT for localized scarf joint interface reinforcement. There were three breakout sets of samples each providing greater than an 11% increase in strength. Two of the breakout sets of test samples were reinforced with bamboo-structured MWCNTs with equal diameters of 30 ± 15 nm and unequal lengths of 1–5 μm for one group and 5–20 μm for the other. The third breakout group was a conventional MWCNT with the same diameter as the bamboo-structured MWCNTs, 30 ±15 nm, and a length of 5–20 μm. The shorter bamboo-structured MWCNT and the conventional CNT displayed twice the amount of modulus increase over the longer bamboo structure. Between the shorter bamboo-structured and the conventional MWCNTs, the conventional MWCNT had the most consistent results which translated to a smaller standard deviation.

Since the conventional MWCNT with a diameter equal to 30 ±15 nm and a length of 5–20 μm achieved one of the highest increases in strength and modulus as well as possessing the most consistent results of all three breakout groups, this type of CNT is ideal for localized reinforcement of a vinyl-ester composite scarf joint. These findings support previous observations of CNT reinforcement that MWCNTs are more ideal for polymer reinforcement due to greater surface area [3].

In general, larger diameter CNTs provided greater strength enhancements compared to single-walled and multi-walled nanotube of a smaller diameter. This is most likely due to the greater surface area of the CNTs with larger diameter. Several interesting observations were apparent when comparing the results of the CNTs with the same diameter of 30 ±15 nm.

When comparing the CNTs with the same 30-nm diameter, the shorter CNTs provoked a higher increase in elastic modulus. The conventional MWCNTs with a diameter of 30 ±15 nm and a length of 1–5 μm produced the greatest increase in elastic modulus with an average enhancement of >26%. This observation held true when both types of 30-nm diameter conventional MWCNTs were compared as well both types of bamboo-structured MWCNTs.

A similar trend was observed while comparing conventional MWCNTs to bamboo-structured CNTs. When the conventional and the bamboo-structured multi-walled CNTs were the exact same size and shape, the modulus of the conventional MWCNT was higher.

This observation supported the findings delineated in a previous study [10]. The study modeled the modulus of an SWCNT for comparison against a similar model for a bamboo-structured SWCNT using molecular dynamics. Although the computer model was developed for single-walled structures only, the conclusions were similar to the comparison between bamboo-structured and conventional MWCNTs observed by this research. The work [10] concluded that the modulus of elasticity was greater for conventional MWCNTs compared to their bamboo-structured counterparts.

As far as the computational modeling was concerned, the global–local model with a discrete resin layer for delamination was useful in predicting the compressive failure strength of the scarf joint. In the model, the fracture mechanics concept was utilized with an initial flaw assumed in the orientation of the scarf taper. The predicted strength based on the energy release rate was within 4% when compared to the average test data. As a result, the computer modeling technique provided acceptable results.

References

1. Mouritz AP, Gellert E, Burchill P, Challis K (2001) Compos Struct 53:21. doi:10.1016/S0263-8223(00)00175-6
2. Thostenson ET, Ren Z, Chou T (2001) Compos Sci Technol 61:1899. doi:10.1016/S0266-3538(01)00094-X
3. Cadek M, Coleman JN, Ryan KP, Nicolosi V, Bister G, Fonseca A, Nagy JB, Szostzk K, Beguin F, Blau WJ (2004) Nano Lett 4(2):353. doi:10.1021/nl035009o
4. Schadler SC, Giannaris SC, Aiayan PM (1998) Appl Phys Lett 73(26):3842. doi:10.1063/1.122911
5. Cooper CA, Cohen SR, Barber AH, Wagner HD (2002) Appl Phys Lett 81(20):3873. doi:10.1063/1.1521585
6. Barber AH, Cohen SR, Wagner HD (2003) Appl Phys Lett 82(23):4140. doi:10.1063/1.1579568
7. Lordi V, Yao N (2000) J Mater Res 15(12):2770. doi:10.1557/JMR.2000.0396
8. Ding F, Bolton K, Rosén A (2006) J Electron Mater 35(2):207. doi:10.1007/BF02692437
9. Greene T (2007) MS Thesis, NPS
10. Kwon YW (2005) In: Schulz MJ, Kelkar A, Sundaresan MJ (eds) Nanoengineering of structural, functional and smart materials. CRC Press, Boca Raton